RSC Advances

PAPER

View Article Online
View Journal | View Issue

Cite this: *RSC Adv.*, 2014, **4**, 50212

Star-like polymer click-functionalized with small capping molecules: an initial investigation into properties and improving solubility in liquid crystals†

James Iocozzia,[a] Hui Xu,[b] Xinchang Pang,[a] Haiping Xia,[b] Timothy Bunning,[c] Timothy White*[c] and Zhiqun Lin*[a]

Received 1st September 2014
Accepted 30th September 2014

DOI: 10.1039/c4ra09597a

www.rsc.org/advances

A novel class of polymer, star-like poly(*tert*-butyl acrylate) (P*t*BA) capped with 4-isocyano-4′-(prop-2-yn-1-yloxy)biphenyl (CNBP), with a well-defined size was synthesized *via* atom transfer radical polymerization (ATRP) and click reaction (*i.e.*, azide–alkyne cyclization). The star-like architecture was composed of 21 separate arms connected to a high-functionality β-cyclodextrin (β-CD) core. The inner star-like P*t*BA blocks were hydrolyzed into poly(acrylic acid) (PAA), yielding star-like CNBP-capped PAA (*i.e.*, star-like PAA-CNBP). The starlike polymers were characterized by gel permeation chromatography (GPC) and dynamic light scattering (DLS) to confirm narrow size distribution, as well as being examined by proton nuclear magnetic resonance (^{1}H-NMR), Fourier transform infrared spectroscopy (FTIR), Raman, and atomic force microscopy (AFM) to verify successful attachment of the click-functionalized capping agent (*i.e.*, CNBP) with structural similarity to low molar mass liquid crystal, 4-cyano-4′-pentylbiphenyl (5CB). Structure and phase behavior were evaluated by AFM and optical imaging. Star-like PAA-CNBP was found to possess improved solubility in a liquid crystal host and interesting surface structures.

Introduction

Thermotropic liquid crystals (LCs) are a well-known class of matter that forms in certain molecular systems between that of a pure liquid and a pure solid.[1,2] LCs are prevalent in many technologies and nature.[3,4] The anisotropy of LC systems, and non-uniform property variations are what make them attractive active media as they selectively respond to myriad perturbations, including deformation, radiation and magnetization.[5] Investigations into the properties of pure or mixed liquid crystalline phases is an ongoing area of research, however the use of LCs as a host species for other chemically-modified active species, such as polymers and nanoparticles, is an emerging area which takes advantage of the unique properties of LCs with the desire to incorporate additional functionality through doping. By far the most common class of material investigated for doping into LCs has been nanoparticles (NPs) of one form or another.[6–13] NPs have been of particular interest because the physics and properties of materials on this scale generally differ from their bulk, macroscopic counterparts.[14,15] Parameters such as size, size distribution, and spatial arrangement greatly affect how NPs respond due to properties such as local surface plasmon resonance (LSPR),[9] quantum confinement,[16] and energy level mixing.[17–19] Research into nanoparticle-liquid crystal composites (NP-LCs) promises a wide spectrum of applications, including advanced display technology,[3,4,20] photonics,[5,21,22] optics,[3,5,17,23] sensors and metamaterials.[3,17] Furthermore, the assembly (self or directed) of NPs has proven to be successful by many other techniques spanning a broad range of disciplines.[24]

One specific area of investigation is the use of LCs as a means of assembling dopant species into various arrangements.[7,8,11,25] The idea being that dopants would align within the LC matrix and have an order to their assembly imposed by the LC host. Unfortunately, the realization of this technique has not been easy. A few active research areas on NPs include gold NPs and quantum dots (QDs) variously passivated with alkylthiolate, alkylthiol, or (*S*)-naproxen ligand species.[7,8,12,13,16,26,27] There are myriad techniques for making NPs (particularly Au,[2,28] Ag,[1] and metal oxides[29]) variably capped with many species in large yield.[8,13] However, some techniques yield NPs with non-uniform size and shapes, while the others cannot afford the synthesis of NPs with tunable size (*i.e.*, limited applicability/variability).[8,30]

[a]*School of Materials Science and Engineering, Georgia Institute of Technology, Atlanta, GA 30332, USA. E-mail: zhiqun.lin@mse.gatech.edu; Fax: +1-404-385-3734; Tel: +1-404-385-4404*

[b]*State Key Laboratory of Physical Chemistry of Solid Surfaces and Department of Chemistry, College of Chemistry and Chemical Engineering, Xiamen University, Xiamen 36105, China*

[c]*Air Force Research Laboratory, Materials and Manufacturing Directorate, Wright Patterson Air Force Base, OH, 45433, USA. E-mail: timothy.white.24@us.af.mil*

† Electronic supplementary information (ESI) available. See DOI: 10.1039/c4ra09597a

Furthermore, the degree and nature of ligand coverage on NPs is oftentimes based on coordination or adsorption rather than strong bonding and subsequent processing steps (sonication, heating, reaction) have the potential to change the surface functionality. This change can affect the solubility, and therefore behavior, interaction, and organization of NPs in LC host media.

The development of well-defined living polymerization techniques such as atom transfer radical polymerization (ATRP)[31–33] in conjunction with star-like polymer templates[34–38] is an interesting alternative with the potential for producing polymeric and nanocomposite systems with improved solubility in LC media. Living polymerization is an expansive class of polymerization techniques in which the polymer chains grow uniformly to yield highly monodisperse (low polydispersity index, PDI) and telechelic (end-reactive) polymers capable of further polymerization/reaction. Pioneered by Matyjaszewski *et al.*,[32,33] ATRP in particular is of great interest because of the retention of end group reactivity, typically halogen atoms which are excellent leaving groups. Thus, the polymeric materials can be further functionalized with methods such as the burgeoning and versatile class of chemistry known generally as "click" chemistry. First reported by Sharpless *et al.*,[39] "click" chemistries are generally characterized as simple and robust addition-type reactions which proceed to high yields at moderate conditions with minimal control of temperature or atmospheric conditions required. Many types of click chemistry have been developed with the azide–alkyne reaction of particular interest in this work.[39–41] More details on the broad field of click chemistry can be found in comprehensive reviews.[42]

Here we report a simple and easily systematized approach for producing functional star-like polymers tethered with small molecules that are structurally similar to the common LC 4-cyano-4′-pentylbiphenyl (5CB). ATRP of *tert*-butyl acrylate (*t*BA) was performed on a 21-arm β-cyclodextrin macroinitiator core to produce starlike poly(*tert*-butyl acrylate) (P*t*BA). In a parallel reaction, a small molecule, 4-isocyano-4′-(prop-2-yn-1-yloxy) biphenyl (CNBP), was synthesized which possessed similar chemical structure to 5CB. Ultimately, CNBP was grafted onto star-like P*t*BA *via* azide–alkyne click chemistry to produce CNBP-capped star-like P*t*BA (*i.e.*, starlike P*t*BA-CNBP) which was subsequently hydrolyzed to yield starlike poly(acrylic acid-CNBP) (PAA-CNBP). The latter can potentially be utilized as template through the coordination interaction between hydrophilic inner PAA blocks and the metal moieties of precursors to produce NPs[43–45] with improved solubility in LC host media as the resulting NPs are intimately and permanently linked with LC-like CNBP.[30] The structural properties were investigated by proton nuclear magnetic resonance (^{1}H-NMR), gel permeation chromatography (GPC), Raman spectroscopy, Fourier transform infrared spectroscopy (FTIR), dynamic light scattering (DLS) and atomic force microscopy (AFM). This simple synthetic approach serves as an initial investigation into the properties and solubility of NP templates (*i.e.*, star-like PAA-CNBP) derived from the β-cyclodextrin core in LC hosts. Moreover, this approach can be readily generalized to investigate a wide range of chemical and physical parameters which influence solubility.

Experimental

Materials

N,*N*,*N*′,*N*″,*N*″-pentamethyldiethylenetriamine (PMDETA, 99%), 2-bromoisobutyryl bromide (2-Br-iBu-Br, 98%), 1-methoxy-2-propanol (M-IPA) (99%), and anhydrous 1-methyl-2-pyrrolidinone (*N*-methyl pyrrolidinone) (NMP) were purchased from Sigma-Aldrich. Sodium azide (99.5%), aluminum oxide (neutral), petroleum ether (60/80), calcium hydride (90–95%), sodium bicarbonate (99%), anhydrous magnesium sulfate (99.5%), hexane, trifluoroacetic acid (99%), and 4-cyano-4′-pentylbiphenyl (5CB) were purchased from Alfa Aesar. Propargyl bromide (99%, stabilized with MgO), and 4-hydroxy-4′-biphenylcarbonitrile were purchased from TCI America. Reagent grade chloroform and ethyl acetate were purchased from BDH. Silica gel (mesh 60–200) was purchased from EMD. All abovementioned chemicals were used as received. β-CD (Sigma-Aldrich) was dried and purified as detailed below. CuBr (98%, Sigma-Aldrich) was purified using a procedure from a previous work.[46] Tertiary butyl acrylate (*t*BA) (99% with 15 ppm 4-methoxyphenol as inhibitor, Alfa-Aesar) was stirred with calcium hydride for 1 h and distilled under heat and light vacuum to remove the inhibitor prior to use. Polyimide (PI-2555) was purchased from HD Microsystems. Norland 68 UV curing glue was purchased from Edmund Optics. Glass rod spacers (10 μm thickness) were purchased from Nippon Electric Glass.

Characterizations

Absolute molecular weights of polymers and their chemical structures were verified by ^{1}HNMR using a Varian VXR-400 (400 MHz) Unity Innova 500 spectrometer equipped with a Nalorac quad-probe. Samples employed $CDCl_3$ as the deuterated solvent with TMS as internal reference. Molecular weight, polydispersity (PDI) and modality of starlike polymers were measured using a Shimadzu gel permeation chromatography setup (GPC equipped with a RID-10A refractive index detector, LC-20A chromatograph pump, and CTO-20A column oven). Tetrahydrofuran (THF) was used as the eluent at an operating temperature of 35 °C and a flow rate of 1 mL min^{-1}. Two 5 μm phenogel 10 E4A columns (molecular weight range: 200 to 2 × 10^6 g mol^{-1}) were calibrated using linear polystyrene (PS) standards. Dipolar functional group incorporation was determined using FTIR. FTIR spectra were measured using a Fisher Thermo Scientific Nicolet 6700 spectrometer equipped with an Ever-Glo source (9600-2 cm^{-1}). FTIR samples were prepared in KBr disks. Morphological properties were investigated with a Bruker Dimension Icon atomic force microscope (AFM) with 36 μm^2 scan areas. Scans were performed in tapping mode at a scanning rate of 0.5 Hz. AFM samples were prepared on cleaned silica substrate (cleaning sequence: water–ethanol–water). Concentrated samples of PAA-CNBP ($c = 0.2$ mg mL^{-1}) were prepared and spin coated at 3000 rpm (Headway Research, model PWM32) for 30 seconds for AFM measurements. Symmetric (polarizable) functional group

incorporation was determined by Stokes-shift Raman scattering. Raman spectra were acquired using a Renishaw inVia Raman microscope equipped with a 785 nm laser (5 mW) and MS20 encoded stage (100 nm resolution) on a Leica DM2500 M microscope. Dynamic light scattering (DLS) was performed using a Wyatt DynaPro NanoStar system at 25 °C using a solid-state 785 nm laser and quartz cuvette.

Preparation of high functionality macroinitiator β-CD-21Br from β-CD-21OH

In a procedure adapted from Pang *et al.*[43] β-CD (5.68 g, 5 mmol) was dried by distilling with toluene at 120 °C to completely remove any water. Once dried, β-CD was dissolved in anhydrous polar solvent 1-methyl-2-pyrrolidinone (60 mL) and chilled to 0 °C in an ice bath. Once cooled, 2-bromoisobutyryl bromide (49 mL, 210 mmol) was added dropwise in a 42 : 1 molar ratio (2-Br-iBu-Br : β-CD-21OH) or equivalently a 2 : 1 molar ratio (2-Br-iBu-Br : –OH) and allowed to react for at least 2 h at low temperature. The reaction was allowed to run an additional 24–36 h to ensure full reactivity of surface –OH groups. The product was then precipitated in hexane under vigorous stirring and allowed to settle overnight. The supernatant was then collected and redissolved in chloroform. The raw product was then added to a separatory funnel and sequentially washed with saturated aqueous sodium bicarbonate ($NaHCO_3$) solution (until no bubbles evolve) and deionized water. Any residual water was removed with $MgSO_4$, and the product was then filtered and dried under vacuum for at least 48 h. The final product was obtained by recrystallization in hexane. Its structure was verified using ^{1}HNMR (solvent $CDCl_3$ δ(ppm)): 1.78 (126H, CH_3), 3.45–5.25 (49H); and FTIR ν(cm^{-1}): 2932 (ν_{C-H}), 1735 ($\nu_{C=O}$), 1159 cm^{-1} (ν_{C-O-C}), 1039 and 1106 (ν_{C-C} coupled with ν_{C-O}). Initiation efficiency (*i.e.*, the conversion of –OH groups to –Br groups) was calculated according to the procedure in our previous work using ^{1}HNMR and was found to be 100%.[46] The same brominated β-CD employed in the previous study was also used in this investigation.

Synthesis of 4-isocyano-4′-(prop-2-yn-1-yloxy)biphenyl small molecule capping agent (CNBP-≡)

Part (I) of Fig. 1 details the synthetic pathway for CNBP-≡. 4-hydroxy-4′-biphenylcarbonitrile (1 g, 5.12 mmol) and potassium carbonate (1.6 g, 25.6 mmol) were added to a 50 mL three-neck flask equipped with a magnetic stirrer and condenser. The atmosphere was exchanged for argon. Anhydrous acetone (10 mL) was then added *via* syringe into the flask and allowed to fully mix for 10 min. Diluted in acetone (5 mL), propargyl bromide (0.7312 g, 6.2 mmol) was added dropwise *via* syringe into the vigorously stirred flask. The flask was then heated to reflux and left to react for 4 days. The raw product was dried for 48 h under vacuum, yielding a bright yellow raw product. It was then dissolved in chloroform and mixed with silica gel until a dry pale yellow colored powder was formed. This was added to a silica gel column prewashed with petroleum ether (PET). A series of solvent mixtures containing petroleum ether (low polarity), ethyl acetate (EtOAc) (medium polarity) and chloroform ($CHCl_3$) (high polarity) were passed through the column, collected, and evaporated. The solvent mixtures were (1 : 0, 1 : 2, 2 : 1, 0 : 1) (PET : $CHCl_3$, v/v); (9 : 1, 4 : 1, 1 : 1) ($CHCl_3$: EtOAc, v/v). The pure product was collected with the solvent mixture 9 : 1 ($CHCl_3$: EtOAc, v/v) ^{1}HNMR (solvent $CDCl_3$ δ(ppm)): 7.60–7.75 (protons from phenylene ring attached cyano group), 7.0–7.6 (protons from phenylene ring attached to oxygen), 4.75 (protons on oxymethylene bridge), and 2.51 (ethynyl proton).

Preparation of 21-arm star-like P*t*BA–Br *via* atom transfer radical polymerization (ATRP)

In a round bottom flask, 200 mL of *t*BA and 20 g of calcium hydride were added. The flask was then attached to a typical distillation setup and allowed to react for approximately 1 h under vigorous stirring (no heat, no vacuum). Then a vacuum and light heat was applied in 5 °C increments until a slow boil was reached. The distillate was collected in a separate container and ready for use. Polymerization of *tert*-butyl acrylate (*t*BA) employed the β-CD-21Br macroinitiator in an ATRP controlled living polymerization. The ATRP synthesis was summarized in part (II) of Fig. 1. A 150 mL threaded cylindrical pressure vessel was sequentially charged with β-CD-21Br (0.1 g), *t*BA (14.3 mL), 2-butanone (14.3 mL) (1 : 1 v/v monomer : solvent), CuBr (0.071 g), and PMDETA (0.1701 g). Upon addition of PMDETA, the contents changed color from a pale, diffuse green to a strong dark green, indicating successful complexation and dispersion of the CuBr/PMDETA co-catalyst. The vessel was then subjected to three freeze–thaw–pump cycles in inert N_2 atmosphere using liquid nitrogen as the freezing agent. The vessel was then set in an oil bath at 90 °C and allowed to react under stirring for 24 h. The raw product was then diluted with acetone to roughly 140 mL total volume and passed through an aluminum oxide column (neutral, pre-washed with acetone) to remove the CuBr salt. The eluent was then precipitated in a mixture of cold methanol and water (1 : 1 v/v). This process was repeated three times to ensure removal of linear homopolymer. The contents were then dried with $MgSO_4$, filtered and dried under vacuum for at least 48 h. ^{1}HNMR (solvent $CDCl_3$ δ(ppm)): 1.35–1.55 (*tert*-butyl protons), 1.25–1.29 (methyl protons on backbone), 2.15–2.35 (proton on tertiary carbon in backbone).

Preparation of azide terminated 21-arm starlike P*t*BA–N_3

Purified 21-arm starlike P*t*BA–Br (1.52 g) was dissolved in dimethylformamide (10 mL) and excess sodium azide (0.7 g) (molar ratio of terminal Br to NaN_3 = 1 : 30) was then added to the reaction flask. The solution was allowed to react for 60 hours at room temperature while covered with aluminum foil. Excess NaN_3 was removed by filtration. The raw product is then precipitated in cold methanol and water (1 : 1, v/v). The precipitate was dissolved in chloroform (30 mL) and washed with deionized water (3 × 15 mL). The organic layer was concentrated to remove $CHCl_3$ and re-dissolved in 100 mL acetone before finally being precipitated in cold methanol and

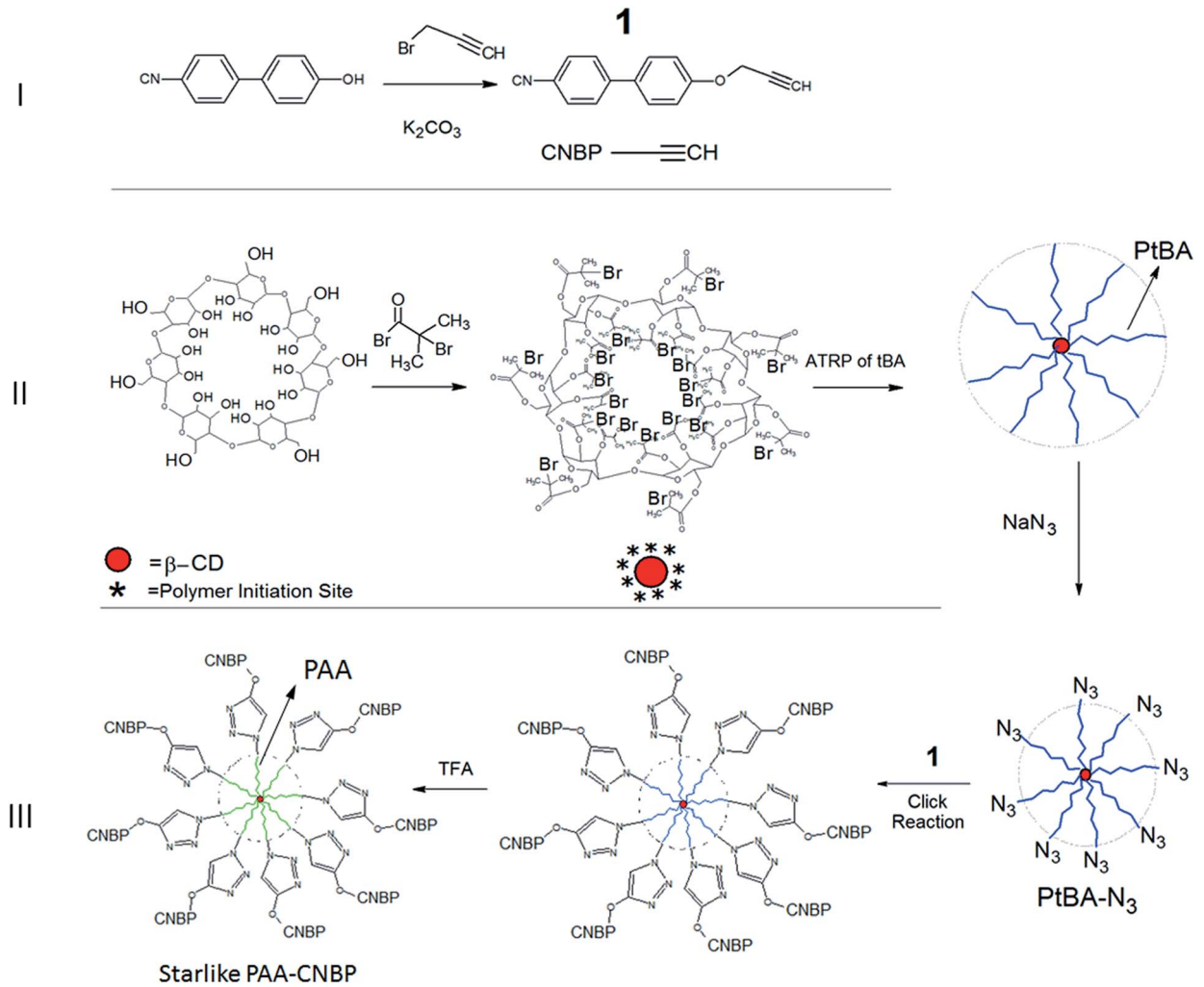

Fig. 1 Reaction schemes for (I) the synthesis of CNBP—≡(1); (II) the synthesis of starlike P*t*BA-Br *via* ATRP; (III) the synthesis of starlike PAA-CNBP *via* click reaction (*i.e.*, azide–alkyne cyclization).

water (1 : 1, v/v). The precipitate was dried in a vacuum oven overnight. Azide functionalization was verified by FTIR $\nu(cm^{-1})$: 2110 ($\nu_{N=N=N}$).

Synthesis of 21-arm starlike PtBA–CNBP by click reaction

Fig. 1 details the synthetic pathway for the click reaction. In a dry 150 mL threaded cylindrical pressure vessel starlike P*t*BA–N_3 (300 mg) and 4-isocyano-4′-(prop-2-yn-1-yloxy)biphenyl (CBNP; 90 mg) were dissolved in DMF (15 mL). To this, CuBr (113.5 mg) and PMDETA (136.8 mg) were added. The vessel was then sealed and subjected to three freeze–pump–thaw cycles under inter N_2 atmosphere using liquid nitrogen as the freezing agent. The contents were then allowed to react at 90 °C for 36 h under stirring in an oil bath. The reaction was quenched by immersing the pressure vessel in liquid nitrogen. The contents were then diluted with THF and passed through an aluminum oxide (neutral) column to remove the copper salt. The product was then precipitated twice in cold methanol and water (1 : 1, v/v) and dried under vacuum at 50 °C for 24 h to yield a slightly yellowish powder.

Hydrolysis of 21-arm starlike P*t*BA-CNBP into 21-arm starlike poly(acrylic acid)-LC

In a 20 mL vial, 21-arm star-like P*t*BA-CNBP (80 mg) was dissolved in dichloromethane (DCM) (12 mL). Next trifluoroacetic acid (4 mL) was added and the solution was stirred for 24 h. 21-arm starlike PAA-CNBP was precipitated out of solution. It was filtered and washed with dichloromethane three times and dried under vacuum for 24 h.

Results and discussion

Synthesis of 4-isocyano-4′-(prop-2-yn-1-yloxy)biphenyl small molecule capping agent (CNBP—≡)

The choice of small molecule capping agent, 4-isocyano-4′-(prop-2-yn-1-yloxy)biphenyl (CNBP), was motivated by its structural similarity and potential for compatibility with the LC host (*i.e.*, 4-cyano-4′-pentyl biphenyl; 5CB). The synthesis of CNBP in a nucleophilic substitution reaction was detailed in reaction pathway I in Fig. 1. Essentially, a terminal alkoxide served as a nucleophile which can attack the methylene carbon of

propargyl bromide with bromine acting as a leaving group. It was necessary to purify the product *via* column chromatography. The eluent ratios used are detailed in the Experimental section. Very fine divisions in polarity of the eluents were required to isolate highly pure final product. Fig. 2 shows the ^{1}H-NMR spectrum of the purified product, verifying the successful alkyne functionalization. The key peaks to note were the alkynyl proton at 2.5 ppm, the two aromatic groupings around 7.8 ppm and 7.05 ppm.

As a verification of alkyne functionalization, Raman spectroscopy was also performed on the capping agent. Raman spectroscopy is complimentary to FTIR in that where one technique affords a weak chemical signature; the other would usually yield a stronger one. Raman gives stronger signals for materials with highly polarizable bonds such as alkenes and alkynes. Fig. 3 shows the Raman spectrum for CNBP—≡ which exhibited the carbon–carbon triple bond vibration mode and the cyano vibration mode at 2127 cm^{-1} and 2226 cm^{-1}, respectively. The relatively weak aromatic peaks were also evident as well as the C–O–C bending mode, which further substantiated that the reaction had occurred (replaced C–O–H bond with C–O–C bond).

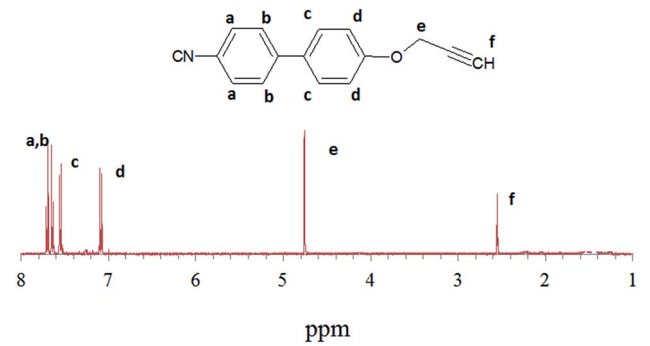

Fig. 2 ^{1}H-NMR spectrum of capping agent (CNBP—≡) (solvent $CDCl_3$). Solvent peaks were removed for clarity.

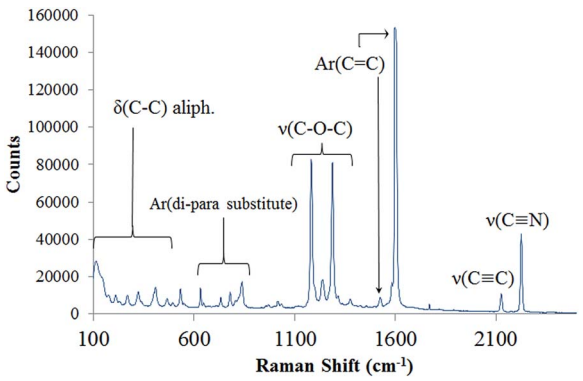

Fig. 3 Raman spectrum of CNBP capping agent. The separate, resolvable signals from the cyano and alkynyl groups were around 2100 cm^{-1}. Aromatic signals indicated the presence of biphenyl component. Laser excitation was at 785 nm.

Preparation of 21-arm starlike PtBA-Br *via* atomic transfer radical polymerization (ATRP)

The synthesis procedure for starlike P*t*BA-Br is depicted in Fig. 1. The 21 hydroxyl groups of β-CD were bromine-functionalized *via* esterification with 2-bromoisobutyryl bromide to yield β-CD-21Br. This served as the macroinitiator for the subsequent polymerization. ATRP was then performed on the macroinitiator through the addition of *tert*-butyl acrylate monomer at a temperature of 90 °C for 24 h (see Experimental section for more details). A CuBr/PMDETA co-catalyst was used for the polymerization. The resulting polymer was first purified several times by fractional precipitation into a 1 : 1 (v/v) mixture of cold methanol and water to remove the linear homopolymer which inevitably formed during ATRP. Fig. 4 describes the GPC traces showing the removal of both the homopolymer peak and the weak shoulder on the main peak. The pure star-like P*t*BA-Br was then characterized by ^{1}H-NMR to obtain an absolute molecular weight. It should be noted that the values obtained from GPC and NMR are not expected to be equal due to the fact that the standards used for calibration were linear PS which possessed different solubility (and favourability) in the eluting solvent (THF) compared to the star-like P*t*BA-Br synthesized herein.

The ^{1}H-NMR spectra of the CNBP capping agent (see Fig. 2 section for more details) and the unfunctionalized starlike P*t*BA are shown in Fig. 5A and B, respectively. Fig. 5C displays a strong signal of the star-like P*t*BA protons which can be integrated. The characteristically strong signal at $\delta = 1.4$ ppm (peak **a**) corresponds to the pendant tertiary butyl protons, and the weaker signal at $\delta = 1$ ppm (peak **b**) can be assigned to the methyl protons at the attachment site on β-CD. The relationship between these respective intensities (normalized to a per proton basis) enabled the length of a single arm to be calculated and thus the total length (*i.e.*, molecular weight) to be determined. It should be noted that only one arm of the star-like polymer is shown in the inset in Fig. 5 for simplicity. In reality there were 21 total polymer arms due to the presence of 21 –OH groups of β-CD capable of reaction.

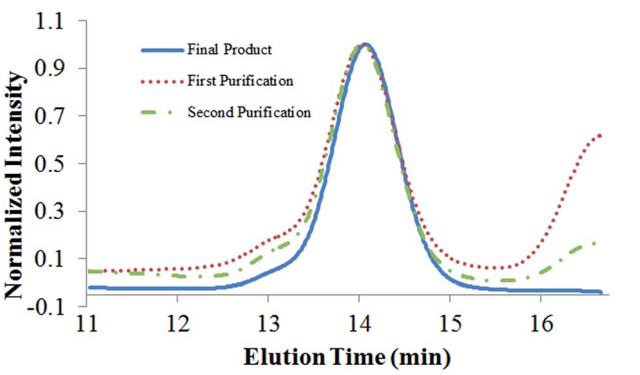

Fig. 4 GPC traces of the star-like P*t*BA-Br in a series of purification steps. Note the removal of the homopolymer (linear P*t*BA) present at long elution times.

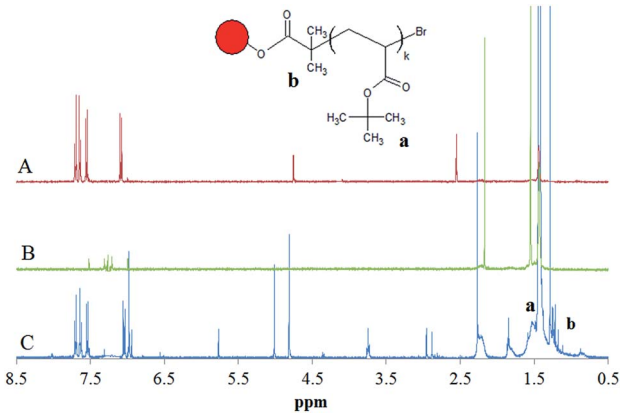

Fig. 5 ^{1}H-NMR spectra of (A) CNBP capping agent (for more detail see Fig. 2), (B) starlike PtBA-Br, and (C) starlike PtBA-CNBP. Inset shows polymer repeat unit (single arm) and proton matching for P*t*BA (solvent $CDCl_3$). Note the combination of the signals from (A) and (B) in the final product (C) particularly in the aromatic region and the shift of the alkynyl proton after the click reaction. The red circle represents the β-CD macroinitiator core. Solvent peaks are removed for clarity.

In addition to the observation of small molecule peaks in the post-click material, a sizeable ppm shift of the alkynyl proton is evident from 2.5 ppm in (A) to 3 ppm in (C). Table 1 summarizes the results of GPC and ^{1}H-NMR analysis. As expected in ATRP, the PDI of the resulting polymer was low, indicating the formation of polymer with narrow molecular weight distribution.

$$M_{n,NMR} = \frac{\left(\frac{A_a}{9}\right)}{\left(\frac{A_b}{6}\right)} \times 21 \text{ arms}$$

where A_a and A_b are the integrated areas of the pendant backbone methyl protons and main-chain methyl protons from Fig. 3C, respectively.

Preparation of azide terminated 21-arm star-like P*t*BA–N_3

The last step in reaction pathway II from Fig. 1 involves the azidation of the terminal bromines of the star-like P*t*BA *via* the reaction with sodium azide (NaN_3). FTIR is a useful technique for verifying the successful azidation of the polymer. This is largely due to the ease with which the dipole moment of the N_3 group can be perturbed. Fig. 6 compares the FTIR spectra of the pre-click (*i.e.*, azide functionalized starlike PAA–N_3) (Fig. 6A)

Table 1 Summary of molecular weights for 21-arm starlike PtBA-Br

Sample	Time (h)	$M_{n,GPC}$[a]	PDI[b]	$M_{n,NMR}$[c]
PtBA-Br	24	108 000	1.07	283 500

[a] The number average molecular weight was determined by GPC with PS calibration standards. [b] Polydispersity index (PDI) was determined by GPC. [c] The number average molecular weight of starlike P*t*BA-Br was determined by ^{1}H-NMR (see Fig. 3C) as follows.

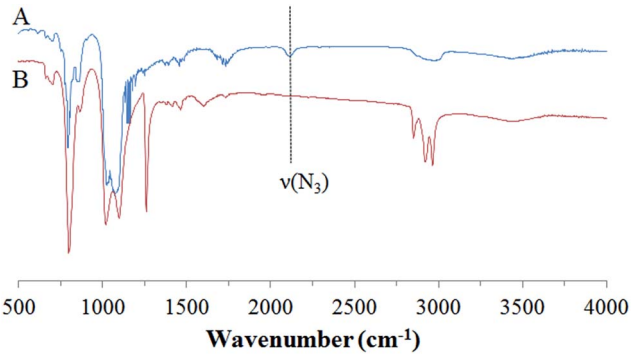

Fig. 6 FTIR spectra of (A) starlike 21-arm PtBA–N_3 and (B) starlike 21-arm PtBA-CNBP. The signal in (A) at 2100 cm^{-1} indicated the presence of azide functionalization. Its disappearance in (B) confirmed the success of the click reaction between azide and alkyne.

and the post-click materials (*i.e.*, after azide has reacted with alkynyl group) (Fig. 6B). The expected stretching signal from $\nu(-N_3)$ was clearly observed at 2103 cm^{-1} in Fig. 6A. The click reaction involved the reaction between a terminal azide group and a terminal alkynyl (triple bond) group. This reaction was highly selective so side reactions were not a concern and it can proceed at moderate conditions of temperature and pressure. After the reaction, a stable 1,2,3-triazole ring was formed (five-membered ring containing three nitrogens and two carbons) which did not have a strong IR signal. Thus, a successful click reaction was evidenced by the disappearance of the azide peak in Fig. 6B.

Characterizations of starlike PAA-CNBP

Successful chemical verification of starlike PAA-CNBP allowed for the characterization of material properties. Several characterization techniques were employed, including AFM, DLS and optical microscopy, to investigate the properties of this novel starlike polymer structure.

Investigation into the morphology formation was undertaken by AFM and summarized in Fig. 7. A sample of starlike PAA-CNBP with a concentration of 0.2 mg mL^{-1} in dimethylformamide (DMF) was prepared and spin-coated on a silicon wafer. The resulting height profile obtained for this sample is shown in Fig. 7A. Forming an interesting interconnected network, the obtained structure was similar in appearance to structures seen in a previous work on high molecular weight comb block copolymers.[47] The similarity of the observed structure as well as the polymeric nature of the system suggested a similar formation mechanism *via* the thin-film dewetting.[47] Initially, the solvent created holes in the thin film of PAA-CNBP as solvent evaporated. The holes then expanded outwards and the rims (*i.e.*, concentrated starlike PAA-CNBP) ahead of the holes eventually merged to form interconnected thread-like structures which cannot propagate further. Notably, despite the different polymer architectures investigated, similar morphologies were observed.[47] A line scan of the interconnected network is shown in Fig. 7B. The average height of the threads was between 2 nm and 3 nm with an average thickness of approximately 6.5 nm.

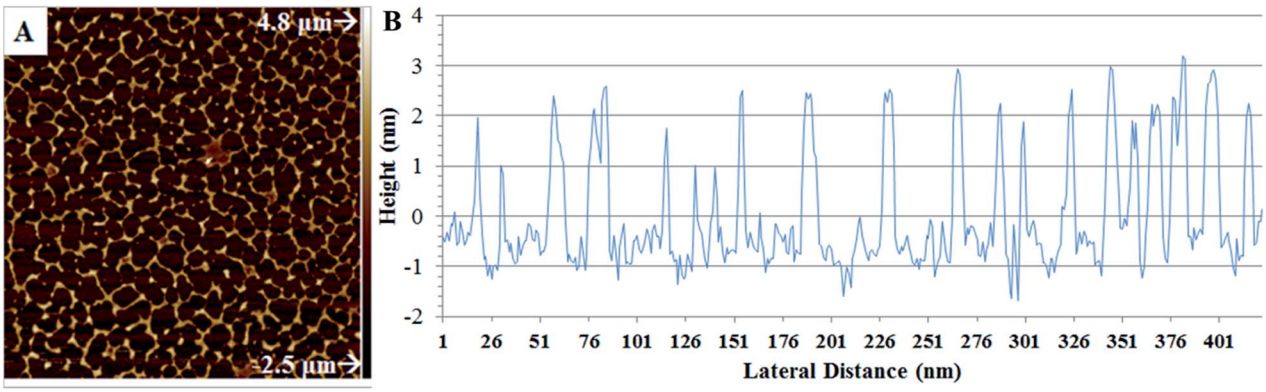

Fig. 7 (A) AFM height image of 21-arm starlike PAA-CNBP. (B) The corresponding cross sectional analysis of starlike PAA-CNBP in (A). Image size = 2.5 × 2.5 μm^2.

Dynamic light scattering (DLS) was also performed on star-like PAA-CNBP at a concentration of 0.2 mg mL^{-1} in methanol (MeOH). Using a multi-arm model, it was found that the peak diameter was approximately 7 nm (Fig. S1†). Comparison between DLS and AFM results was challenging given that the structures observed in the latter were more complicated assemblies of individual star polymers, and thus the larger dimensions. However, DLS did verify the production of low polydispersity star polymer, which is a conclusion also supported by GPC and typical of controlled living polymerizations.

The solubility of the star-like PAA-CNBP in the LC host (*i.e.*, 5CB) was also investigated in two ways. First, samples with from concentrations from approximately 0.3 wt% to 1.76 wt% of PAA-CNBP in 5CB were prepared. The choice of 5CB as the LC host was due to its structural similarity to the capping agent decorating the star-like PAA-CNBP. Table S1† summarizes the different concentrations prepared and their corresponding digital images of the various doped LC samples are shown in Fig. S2.† Samples were heated to 60 °C (above the nematic-to-isotropic transition temperature T_{NI} of 5CB) and sonicated for 5 min. Images of samples A–H were obtained in both the isotropic and nematic states of the 5CB host. It was found that both the isotropic and nematic states for sample A, B, and C yielded clear solutions which were stable after several hours, exhibiting minimal sedimentation of the star-like PAA-CNBP. These corresponded to a peak wt% of 0.72 which was fairly high loading for such systems. Above 0.72 wt% loadings, sedimentation was clearly observed (samples D through H) in Fig. S2† in both the isotropic and nematic phases (circled regions). Another notable observation is that even the isotropic phases at higher loading were cloudier, likely indicating a dispersion of the star-like PAA-CNBP in the 5CB host due to thermal and sonic agitations. Additional investigations into the behaviour in other LC hosts are necessary to better understand the solubility behaviour.

Conclusions

Through a combination of controlled/living polymerization (*i.e.*, ATRP) and click chemistry (*i.e.*, azide–alkyne cyclization), a novel star-like PAA-CNBP composed of inner hydrophilic PAA blocks and outer small molecules (*i.e.*, CNBPs) that possessed similar chemical structures to the small molecular LC host (*i.e.*, 5CB) were synthesized. The uniformity of the resulting star-like polymer was verified by GPC and DLS. The success of click functionalization was verified by ^{1}H-NMR, FTIR, and Raman measurements. The properties of the starlike PAA-CNBP were investigated by AFM and optical imaging. An interesting interconnected morphology was formed, analogous to prior examinations of high molecular weight comb block copolymers. In addition, the star-like PAA-CNBP demonstrated solubility in the canonical nematic liquid crystal host 5CB up to 0.72 wt%. We expect that investigations into the variation of key parameters including the molecular weight of inner polymer blocks, the type of capping agent, and the length of capping agent may increase the solubility of the nanoparticles and facilitate a better understanding of the observed structure and phase behavior. These star-like PAA-CNBP can be employed as templates to produce NPs intimately and permanently connected with CNBP that render the improved solubility in the LC host. The CNBP-capped NPs would be formed *via* the coordination interaction between hydrophilic inner PAA block and the metal moieties of precursors.[43] The ability to harness the dynamism of the LC phase to deliberately and repeatedly control the arrangement of functional nanoscale materials (*e.g.*, NPs, nanorods, *etc.*) is the key to enabling for applications in sensing, photonics and flexible electronics among others.

Acknowledgements

This work was financially supported by Air Force Office of Scientific Research (FA9550-09-1-0162; BIONIC Center seed grant). TJW and TJB acknowledge the financial support of AFOSR and the Air Force Research Laboratory.

Notes and references

1 E. R. Zubarev, S. A. Kupstov, T. I. Yuranova, R. V. Talroze and H. Finkelmann, *Liq. Cryst.*, 1999, **26**, 1531–1540.
2 E. R. Zubarev, R. V. Talroze, T. I. Yuranova, N. A. Plate and H. Finkelmann, *Macromolecules*, 1998, **31**, 3566–3570.
3 *Liquid Crystals: Frontiers in Biomedical Applications*, ed. S. J. Woltman, G. D. Jay and G. P. Crawford, World Scientific Publishing Co. Pte. Ltd, 2007.
4 H. Qi and T. Hegmann, *J. Mater. Chem.*, 2008, **18**, 3288–3294.
5 J. P. F. Lagerwall and G. Scalia, *Curr. Appl. Phys.*, 2012, **12**, 1387–1412.
6 R. Basu and G. Iannacchione, *Phys. Rev. E: Stat., Nonlinear, Soft Matter Phys.*, 2009, 80.
7 R. Bitar, G. Agez and M. Mitov, *Soft Matter*, 2011, **7**, 8198–8206.
8 M. Draper, I. M. Saez, S. J. Cowling, P. Gai, B. Heinrich, B. Donnio, D. Guillon and J. W. Goodby, *Adv. Funct. Mater.*, 2011, **21**, 1260–1278.
9 L. S. Hirst, J. Kirchhoff, R. Inman and S. Ghosh, in *Emerging Liquid Crystal Technologies V*, ed. L. C. Chien, Spie-Int Soc Optical Engineering, Bellingham, 2010, vol. 7618.
10 M. Mitov, C. Bourgerette and F. de Guerville, *J. Phys.: Condens. Matter*, 2004, **16**, S1981–S1988.
11 J. C. Payne and E. L. Thomas, *Adv. Funct. Mater.*, 2007, **17**, 2717–2721.
12 H. Qi and T. Hegmann, *J. Mater. Chem.*, 2006, **16**, 4197–4205.
13 U. Shivakumar, J. Mirzaei, X. Feng, A. Sharma, P. Moreira and T. Hegmann, *Liq. Cryst.*, 2011, **38**, 1495–1514.
14 *Handbook of Nanophysics: Nanoparticles and Quantum Dots*, ed. K. D. Sattler, CRC Press, 2011.
15 *Handbook of Nanophysics: Principles and Methods*, ed. K. D. Sattler, CRC Press, 2011.
16 M. Z. Zhu, H. F. Qian, X. M. Meng, S. S. Jin, Z. K. Wu and R. C. Jina, *Nano Lett.*, 2011, **11**, 3963–3969.
17 B. Kinkead and T. Hegmann, *J. Mater. Chem.*, 2010, **20**, 448–458.
18 J. M. Slocik, A. O. Govorov and R. R. Naik, *Nano Lett.*, 2011, **11**, 701–705.
19 M. Tamborra, M. Striccoli, R. Comparelli, M. L. Curri, A. Petrella and A. Agostiano, *Nanotechnology*, 2004, **15**, S240–S244.
20 H. Qi, B. Kinkead and T. Hegmann, *Adv. Funct. Mater.*, 2008, **18**, 212–221.
21 H. S. Oh, S. Liu, H. Jee, A. Baev, M. T. Swihart and P. N. Prasad, *J. Am. Chem. Soc.*, 2010, **132**, 17346–17348.
22 M. Z. Alam, T. Yoshioka, T. Ogata, T. Nonaka and S. Kurihara, *Chem.–Eur. J.*, 2007, **13**, 2641–2647.
23 A. Christofi, N. Stefanou, G. Gantzounis and N. Papanikolaou, *J. Phys. Chem. C*, 2012, **116**, 16674–16679.
24 M. Grzelczak, J. Vermant, E. Furst and L. Liz-Marzan, *ACS Nano*, 2010, **4**, 3591–3605.
25 D. Coursault, J. Grand, B. Zappone, H. Ayeb, G. Levi, N. Felidj and E. Lacaze, *Adv. Mater.*, 2012, **24**, 1461–1465.
26 C. Gautier and T. Burgi, *Chemphyschem*, 2009, **10**, 483–492.
27 B. Kinkead and T. Hegmann, *J. Mater. Chem.*, 2010, **20**, 448.
28 *Thermal Analysis of Polymers*, ed. J. D. Menczel and R. B. Prime, Wiley, Hoboken, NJ, 2009.
29 J. Fan, S. W. Boettcher and G. D. Stucky, *Chem. Mater.*, 2006, **18**, 6391–6396.
30 X. C. Pang, L. Zhao, W. Han and Z. Lin, *Nat. Nanotechnol.*, 2013, **8**, 426–431.
31 H. Gao and K. Matjaszewski, *Macromolecules*, 2006, **39**, 4960–4965.
32 *Controlled/Living Radical Polymerization: From Synthesis to Materials*, ed. K. Matyjaszewski, Oxford University Press, 2006.
33 *Controlled/Living Radical Polymerization: Progress in RAFT, DT, NMP, & OMRP*, ed. K. Matyjaszewski, Oxford University Press, 2006.
34 K. Ohno, B. Wong and D. Haddleton, *J. Polym. Sci., Part A: Polym. Chem.*, 2001, **39**, 2206–2214.
35 X. W. Fan, L. J. Lin and P. B. Messersmith, *Compos. Sci. Technol.*, 2006, **66**, 1198–1204.
36 Q. Zhang, L. Guang-Zhao, B. Remzi and D. Haddleton, *Chem. Commun.*, 2012, **48**, 8063–8065.
37 Y. Miura, A. Narumi and S. Matsuya, *J. Polym. Sci., Part A: Polym. Chem.*, 2005, **43**, 4271–4279.
38 J. S. Li, H. N. Xiao and Y. S. Kim, *J. Polym. Sci., Part A: Polym. Chem.*, 2005, **43**, 6345–6354.
39 H. C. Kolb, M. G. Finn and K. B. Sharpless, *Angew. Chem., Int. Ed.*, 2001, **40**, 2004–2021.
40 V. D. Bock, H. Hiemstra and J. H. van Maarseveen, *Eur. J. Org. Chem.*, 2006, 51–68.
41 K. Kempe, A. Krieg, C. R. Becer and U. S. Schubert, *Chem. Soc. Rev.*, 2012, **41**, 176–191.
42 J. E. Moses and A. D. Moorhouse, *Chem. Soc. Rev.*, 2007, **36**, 1249–1262.
43 X. C. Pang, L. Zhao, W. Han, X. K. Xin and Z. Q. Lin, *Nat. Nanotechnol.*, 2013, **8**, 426–431.
44 E. J. Tang, G. X. Cheng, X. L. Ma, X. S. Pang and Q. Zhao, *Appl. Surf. Sci.*, 2006, **252**, 5227–5232.
45 X. Pang, C. Feng, H. Xu, W. Han, X. Xin, H. Xia, F. Qiu and Z. Lin, *Polym. Chem.*, 2014, **5**, 2747–2755.
46 X. C. Pang, L. Zhao, M. Akinc, J. K. Kim and Z. Q. Lin, *Macromolecules*, 2011, **44**, 3746–3752.
47 L. Zhao, M. Goodman, N. Bowden and Z. Lin, *Soft Matter*, 2009, **5**, 4698–4703.